Secure Optical Communication Based on Common-Injection-Induced Synchronization of Wideband Complex Signals

Anke Zhao, Ning Jiang,* Shiqin Liu, Yiqun Zhang, Kun Qiu
School of Information and Communication Engineering, University of Electronic Science and Technology of China, Chengdu 611731, China
** uestc_nj@uestc.edu.cn*

Abstract: We propose and experimentally demonstrate a novel secure optical communication scheme that supports high encryption efficiency and high-speed transmissions over Gbit/s with satisfactory BER performance, by achieving common-injection-induced synchronization between two wideband complex entropy sources.
OCIS codes: (060.2330) Fiber optics communications; (060.4785) Optical security and encryption; (140.154) Chaos.

1. Introduction

Since the first demonstration of chaos synchronization by Pecora and Carroll [1], chaotic systems have been widely applied in secure optical communications [2-4]. The noise-like and unpredictability characteristics of chaotic signal make it sufficient to hide the message and realize secure transmission. However, the practical applications of chaos source generated by external-cavity semiconductor laser (ECSL) are limited by two aspects. On one hand, chaotic intensity oscillation is dominated by the intrinsic laser relaxation oscillation, resulting in that the effective bandwidth of chaotic signal is limited. As a result, this restricts the signal transmission capacity of optical chaos-based secure communication systems. On the other hand, in ECSL systems, the external cavity resonance induces a periodic modulation pattern in the power spectrum, which results in an obvious time delay signature (TDS) in the generated chaos. The TDS can be easily identified by several methods, such as the autocorrelation function (ACF), the digital mutual information (DMI), and the spectrum analysis [5], which threatens the security of chaos communications. Once the eavesdropper figures out the feedback delay time, the chaotic system may be reconstructed using the same hardware parameters. The exposure of TDS would degrade the randomness and complexity of the chaotic source. Therefore, to improve the practical performance of ECSL-generated chaos in secure optical communications, it is important to simultaneously achieve the bandwidth enhancement and the TDS suppression for optical chaos source.

In this work, we experimentally demonstrate a novel method to generate synchronized wideband complex signals and its application in secure optical communications. In the proposed system, two conventional ECSLs subject to a common injection light are firstly utilized to generate synchronized chaos in two communication parties. Then the local chaotic signals are used as the driving signals to generate synchronized wideband complex carriers, in virtue of the spectrum expansion effect of chaotic phase-modulation and the phase-to intensity conversion effect of dispersive component. Based on the synchronized wideband complex carrier generation, high-security message transmission with a bit rate over Gb/s and satisfactory BER performance is achieved.

2. Experimental setup

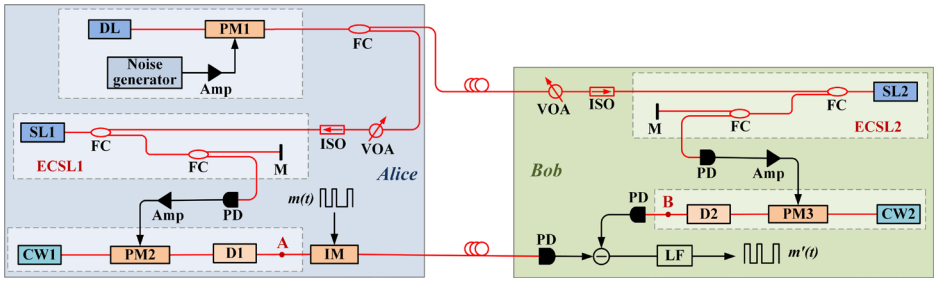

Fig. 1. Experimental setup of the proposed secure optical communication system; DL, drive laser, SL, slave laser, PM, phase modulator; FC, fiber coupler; PD, photodetector; Amp, RF amplifier; VOA, variable optical attenuator; M, mirror; ISO, optical isolator; D1 and D2, dispersive components; IM, intensity modulator; LF, low-pass filter; *m(t)*: original message; *m'(t)*: recovery message.

The experiment setup for the proposed secure optical communication system is shown in Fig. 1. A closed-loop configuration under common unidirectional injection is used to obtain the chaotic driving signals. Specifically, a constant-amplitude random-phase (CARP) signal generated by modulating a CW laser referred to as drive laser (DL) with a noise phase is equally split and then injected into two ECSLs (ECSL1 and ECSL2) deployed at two users (Alice and Bob). Specifically, a 25-Gb/s arbitrary waveform generator is employed to output a white Gaussian noise signal for the RF input of the phase modulator PM1. The CARP signal outputted from PM1 is equally split by a 50:50 fiber coupler (FC), then passed through optical isolators (ISO) and variable optical attenuators (VOAs), and finally injected

into the local ECSLs. The operation wavelength of DL is set at 1549.6 nm, and the frequency detuning between DL and the local ECSLs is 9.3 GHz. The feedback strength and the corresponding feedback delay of ECSL1 (ECSL2) are -20dB and 82.78 ns, respectively. The emissions of two local continuous-wave lasers CW1 (Alice end) and CW2 (Bob end) are sent into two phase modulators PM2 and PM3, respectively. The RF driving signals of PM2 and PM3 are the chaotic outputs of the local ECSLs after photon-detection by photodetectors (PDs) and amplification by RF amplifiers. The chaotic-phase-modulated lights are subsequently passed through two dispersive components (D1 and D2) to generate wideband complex signals at positions A and B, respectively. At the transmitter (Alice), the message is embedded into the carrier through an intensity modulator with a 3-dB bandwidth of 10 GHz. At the receiver (Bob), the message is recovered by the subtraction of the local wideband complex carrier generated at Bob from the encoded transmitted signal. Here these two wideband complex carriers are collected by an oscilloscope with which the synchronization and the subtraction are performed. The recovered message is subsequently filtered by a low-pass four-order Butterworth filter with a cut-off frequency of 0.8R, where R is the bit rate of message. In our experiment, two 50-km single-mode fibers (SMFs) with a dispersion coefficient of 16 ps/nm/km are adopted as the dispersive components, which can also be replaced by fiber gratings or dispersion compensation fibers. The central wavelengths of theCW1 and CW2 are set to 1550 nm. The bandwidths of the phase modulators are 20 GHz, with a half-wave voltage of 3.8 V. The bandwidths of all PDs are 30 GHz. The peak-to-peak amplitude of the driving signals of PM2 and PM3 are limited at 6.1 V. The power gains of the RF amplifiers are 35 dB. All the electronic signals are detected, measured, and recorded by a 100 GS/s digital oscilloscope with four 25-GHz bandwidth channels.

3. Results and analyses

Fig. 2 illustrates the results in terms of the time series, power spectra and ACF traces for the chaotic driving signal generated from ECSL1 (first column) and the carrier signal (second column) measured at Alice end (refer to position A in Fig. 1). Here, the effective bandwidth is adopted to quantify the bandwidth characteristic, which is defined as the span between direct current (DC) component and the frequency where 80% of energy is contained in the RF spectrum [5]. The power spectra are computed from the time domain signals which are recorded by the oscilloscope, based on fast Fourier transform (FFT). It is observed that the power spectrum of the output signal [Fig. 2(d)] is greatly expanded and is much flatter than that of the initial chaos generated by ECSL1 [Fig. 2(c)]. The effective bandwidth of the chaotic driving signal is only 10.6 GHz, while for the carrier signal at position A the effective bandwidth is 21.85GHz which is larger than twice of the effective bandwidth of the initial chaos. The bandwidth enhancement is attributed to the combined effects of PM-induced spectrum expansion and SMF-induced phase-to-intensity conversion [7]. On the other hand, the ACF curve of the initial chaos is depicted in Fig. 2(e), where an obvious peak appears at the position of feedback delay, which means that the TDS can be easily identified. However, for the carrier signal at position A, as shown in Fig. 2(f), no distinguishable peak appears at the position nearby the feedback delay in the ACF trace, the TDS is completely suppressed under the joint nonlinearity effects of the chaotic phase modulation and the dispersive fiber. In addition, the elimination of TDS also means that the complexity of chaos is greatly enhanced [8]. It is worth mentioning that the results for the carrier (at position B) generated at Bob end are much similar to these of Alice shown here, for the sake of simplicity, we do not show them here.

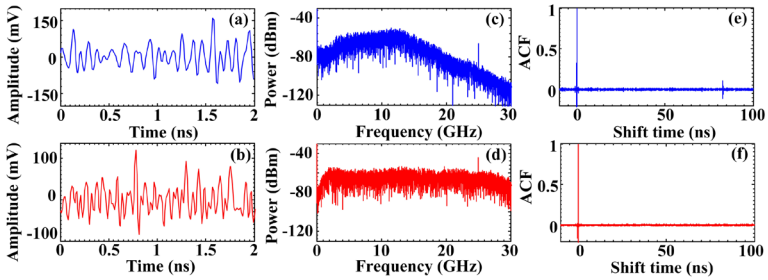

Fig. 2. Temporal intensity waveforms (first column), power spectra (second column) and ACF traces (third column) of the chaotic driving signal generated by ECSL1 (first row) and the carrier signal measured at position A in Fig. 1 (second row).

Figure 3 illustrates the temporal waveforms of the carrier signals measured at the positions A and B in Fig. 1, as well as the corresponding correlation plots between them. Here the cross-correlation coefficient (CC) defined in [6] is adopted to quantify the synchronization quality. It is shown that the temporal waveforms of the two carrier signals [Figs. 3(a) and 4(b)] exhibit almost the same fluctuations, the CC value between them is 0.942, this indicates that high-quality synchronization is achieved between the wideband complex carriers [Fig. 3(d)]. While the CC value between the CARP injection and the carrier signal measured at position A is only 0.016 [Fig. 3(d)], which means that the generated carrier is incoherent with the CARP injection. Similar phenomenon is also observed in the correlation plot between the CARP injection and the carrier signal at Bob end (position B), which is not presented here for simplicity. Since in the proposed system only the common CARP injections are transmitted over the public link, the

generations of the local wideband complex carriers are private, which guarantees high security for the message transmission between Alice and Bob.

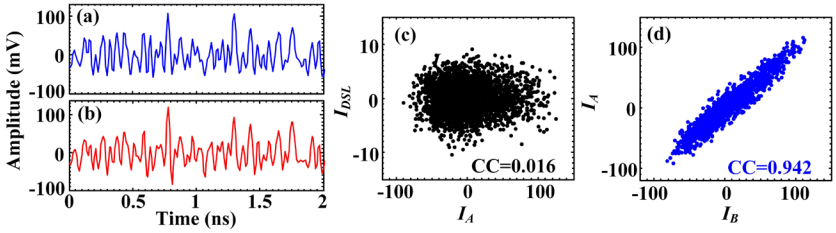

Fig. 3. The temporal waveforms of the output signals measured at positions (a) A and (b) B in Fig. 1, as well as the corresponding correlation plots (c) between the CARP injection and the carrier signal at positions A, (d) between the two carrier signals.

Figure 4 demonstrates the application of the proposed wideband complex signals in secure optical communication for the case of back-to-back transmission. The original message signal with a bit rate of 5 Gb/s is directly measured by oscilloscope as shown in the black line of Fig. 4(a), while the recovered message is depicted in the red line. The comparison between the original message signal and the recovered message signal indicates that the message is correctly recovered, which is further evidenced by the eye diagram of the recovered message as shown in Fig. 4(c). Regarding the corresponding encrypted signal as illustrated in Fig. 4(b), the temporal waveform exhibits a noise-like characteristic with randomly oscillating intensity, indicating that the message signal is well hidden in the carrier. Here we consider a possible attack scenario namely direct detection with linear filtering (DDLF) [4]. In this attack method, the eavesdropper directly detects the encrypted signal from the public link by PD and then adopts a filter with a cutoff frequency equaling the message bit rate to recover the message. Fig. 4(e) illustrates the BER performances of the encrypted, the decrypted and the intercepted messages as a function of the message bit rate. Here 2×10^6 bits are used to calculate the BER, by comparing the recovered message with the original one. For the legal recovered message, the BER is always below 3.8×10^{-3}, which is the hard decision forward error correction (HD-FEC) threshold. It is indicated that the good synchronization performance of the wideband physical sources make it is possible to encrypt the message with a bit rate over 10 Gb/s. By contrast, the BER for the encrypted message and intercepted message are much higher than that of the legal recovered message, and the message cannot be recovered by the DDLF attack with a BER of over 10^{-2}, when the bit rate is larger than 4 Gb/s.

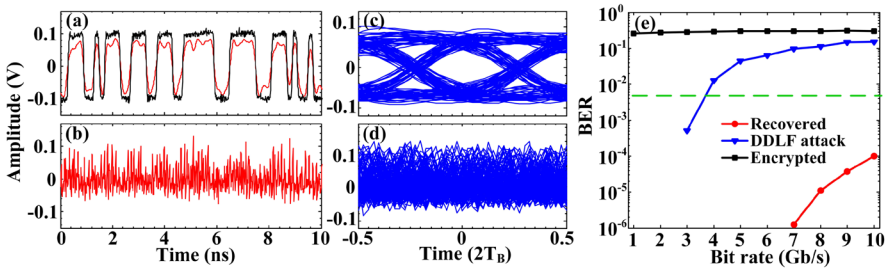

Fig. 4. Temporal intensity waveforms of (a) the original message (black) and the recovered message (red), (b) the encrypted message. The eye diagrams of (c) the recovered message and (d) the encrypted message. (e) BER performances of the encrypted message (black), the recovered message (red) and the intercepted message (blue), as a function of the message rate. The green dashed line denotes the threshold of HD-FEC.

4. Conclusion

In conclusion, a novel scheme for achieving high-speed secure optical communication has been proposed and experimentally demonstrated, based on the synchronization of wideband complex sources. In the proposed scheme, two synchronized wideband TDS-suppressed outputs are independently generated from the initial chaotic driving signals in two communication parties. The high-quality synchronization with a large CC value of 0.942 enables the proposed wideband complex sources to encrypt and decrypt message. The communication performance is investigated in back-to-back transmission case, which indicates that the message can be correctly recovered at the receiver, and cannot be recognized by the eavesdropper. The results indicate that the wideband carrier enables the secure transmission of 10 Gb/s signal, and the elimination of TDS for the carrier can enhance the complexity and communication security.

5. Reference

[1] M. Pecora, et al., Phys. Rev. Lett. **64**, 821-825 (1990).
[2] A. Argyris, et al., Nature **438**, 343–346 (2005).
[3] M. Sciamanna, et al., Nat. Photonics **9**, 151–162 (2015).
[4] N. Jiang, et al., Opt. Lett. **44**, 1536–1539 (2019).
[5] S. Y. Xiang, et al., J. Lighw. Technol. **34**, 4221–4227 (2016).
[6] T. Sasaki, et al., Opt. Express **25**, 26029–26044 (2017).
[7] A. K. Zhao, et al., J. Lighw. Technol. **37**, 5132–5139 (2019).
[8] D. Rontani, et al., Opt. Lett. **41**, 4637–4640 (2016).